THE JOURNAL OF BIOLOGICAL CHEMISTRY VOL. 286, NO. 41, pp. 35380–35387, October 14, 2011

The USP19 Deubiquitinase Regulates the Stability of c-IAP1 and c-IAP2*[S]

Received for publication, July 12, 2011, and in revised form, August 12, 2011 Published, JBC Papers in Press, August 17, 2011, DOI 10.1074/jbc.M111.282020

Yide Mei[‡§1], **Allison Alcivar Hahn**[‡1,2], **Shimin Hu**[‡3], **and Xiaolu Yang**[‡4]

From the [‡]*Department of Cancer Biology and Abramson Family Cancer Research Institute, Perelman School of Medicine, University of Pennsylvania, Philadelphia, Pennsylvania 19104 and the* [§]*School of Life Sciences, University of Science and Technology of China, Hefei, Anhui 230027, China*

The inhibitors of apoptosis (IAPs) are critical regulators of apoptosis and other fundamental cellular processes. Many IAPs are RING domain-containing ubiquitin E3 ligases that control the stability of their interacting proteins. However, how IAP stability is regulated remains unclear. Here we report that USP19, a deubiquitinating enzyme, interacts with cellular IAP 1 (c-IAP1) and c-IAP2. Knockdown of USP19 decreases levels of both c-IAPs, whereas overexpression of USP19 results in a marked increase in c-IAP levels. USP19 effectively removes ubiquitin from c-IAPs *in vitro*, but it stabilizes c-IAPs *in vivo* mainly through deubiquitinase-independent mechanisms. The deubiquitinase activity is involved in the stabilization of USP19 itself, which is facilitated by USP19 self-association. Functionally, knockdown of USP19 enhances TNFα-induced caspase activation and apoptosis in a c-IAP1 and 2-dependent manner. These results suggest that the self-ubiquitin ligase activity of c-IAPs is inhibited by USP19 and implicate deubiquitinating enzymes in the regulation of IAP stability.

The inhibitors of apoptosis (IAPs)[5] were initially identified as baculovirus-encoded products that prevent apoptosis of infected insect cells (1, 2). The cellular homologues of baculoviral IAPs have since been found in a wide range of organisms and are involved in both apoptotic and non-apoptotic processes (3–6). The function of IAPs is largely governed by two zinc-binding domains: the baculoviral IAP repeat (BIR) and the really interesting new gene (RING) domains. Each IAP has at least one copy, and often three tandem copies, of the BIR domain, the signature motif of this family. BIR domains and the flanking sequences mediate the interaction of IAPs with their target proteins. The RING domain, which is present in about half of all mammalian IAPs, endows these IAPs with the ubiquitin E3 ligase activity and determines the consequence of these interactions (4, 7–9). For apoptosis regulation, the BIR domains and the flanking regions of some IAPs, particularly the mammalian X-linked IAP (XIAP) and the *Drosophila* IAP1, directly bind to and inhibit caspases (10), the apoptotic proteases that orchestrate the initiation and execution of apoptosis (11, 12). The E3 ligase activity of XIAP and *Drosophila* IAP1, which mediates proteasomal degradation of caspases, is further needed for effective suppression of apoptosis (13, 14).

The functions of IAPs are nevertheless diverse. In this context, the most extensively investigated IAPs are perhaps the mammalian cellular IAP 1 (c-IAP1) and c-IAP2. c-IAPs share high sequence similarity and were initially identified as part of the intracellular signaling complex that is formed following activation of the tumor necrosis factor receptor (15). Unlike XIAP, c-IAP1 and c-IAP2 exhibit minimal binding to caspases and may not play an important role in the inhibition of these proteases. c-IAPs do interact with a multitude of overlapping and distinct substrates, including those involved in apoptosis, NF-κB signaling, and oncogenesis, and mediate the ubiquitination of these substrates through their robust ubiquitin E3 ligase activity (7–9). c-IAPs ubiquitinate Smac/DIABLO, a mitochondrial protein released to the cytoplasm on apoptosis induction (16, 17), and target it for proteasomal degradation leading to apoptosis inhibition (9). In the canonical NF-κB pathway activated by TNFα, c-IAP1 and c-IAP2 promote K63 poly-ubiquitination of RIP1, which enhances NF-κB activation (18, 19). By contrast, in the non-canonical NF-κB pathway, c-IAPs are responsible for the ubiquitination and degradation of NF-κB-inducing kinase with the consequential attenuation of NF-κB activation (20–23). The importance of c-IAPs in human disease is highlighted by the involvement of c-IAP2 in mucosa-associated lymphoid tissue (MALT) lymphoma, the most common type of human lymphoma that arises in extranodal sites (24). A high percentage of MALT lymphomas express a c-IAP2-MALT1 fusion protein generated by the t(11;18) chromosomal translocation. The target of c-IAP2 related to MALT lymphomas is likely Bcl10, an essential component for antigenic signaling to NF-κB (25, 26). Regulation of Bcl10 by c-IAP2 is disrupted in cells with the c-IAP2-MALT fusion protein (25, 26), which may contribute to hyperactive NF-κB and uncontrolled B-cell proliferation. Although this func-

* This work was supported, in whole or in part, by National Institutes of Health Grants CA108872 and GM060911. This work was also supported by a Leukemia & Lymphoma Society Scholar award (to X. Y.).

[S] The on-line version of this article (available at http://www.jbc.org) contains supplemental Figs. S1–S3.

[1] Both authors contributed equally to this work.

[2] Present address: Illumina, Inc., San Diego, CA 92121.

[3] Present address: Dept. of Hematopathology, University of Texas M. D. Anderson Cancer Center, Houston, TX 77030.

[4] To whom correspondence should be addressed: 421 Curie Blvd., Room 610, BRBII/III, Philadelphia, PA 19104-6160. Tel.: 215-573-6739; Fax: 215-573-6725; E-mail: xyang@mail.med.upenn.edu.

[5] The abbreviations used are: IAP, inhibitor of apoptosis; c-IAP, cellular IAP; ALLN, *N*-acetyl-Leu-Leu-nor-Leu-al; BIR, baculoviral IAP repeat; DUB, deubiquitinating enzyme; MALT, mucosa-associated lymphoid tissue; RING, really interesting new gene; XIAP, X-linked IAP; USP, ubiquitin-specific protease; UBP, ubiquitin-specific processing protease; CA, mutation of Cys to Ala.

tion implied a role for c-IAP2 in tumor suppression, the importance of c-IAP1 in tumorigenesis is suggested by its overexpression in certain human tumors and by its ability to target the c-Myc inhibitor Mad1 for proteasomal degradation (27).

c-IAPs also regulate their own levels or each other's through their ubiquitin E3 activity. c-IAPs, as well as XIAP, undergo self-ubiquitination and proteasomal degradation during glucocorticoid-induced T-cell death (7). Binding to Smac can also induce c-IAP self-ubiquitination and degradation (28). In addition, c-IAP1 promotes the degradation of c-IAP2 via ubiquitination (29, 30). Of note, small compound Smac mimetics prompt the degradation of c-IAP1 and c-IAP2, causing NF-κB-mediated TNFα production and subsequent TNFα-dependent apoptosis in certain tumor cells (20, 21, 31, 32). Smac mimetics are currently in preclinical and clinical tests for cancer therapy (6, 33).

Despite increasing knowledge on c-IAP-mediated degradation of various target proteins, how self-ubiquitination of c-IAPs is normally prevented remains poorly understood. Protein ubiquitination is a reversible process, and increasing evidence indicates the importance of deubiquitinating enzymes (DUBs) in ubiquitin-dependent pathways (34, 35). Two major classes of DUBs have been identified, the ubiquitin C-terminal hydrolases and ubiquitin-specific processing proteases (UBPs), both of which are cysteine proteases. Although ubiquitin C-terminal hydrolases are relatively small in size and release ubiquitin from its precursors and small adducts, UBPs are large proteins and remove ubiquitin from poly-ubiquitinated proteins. One of the UBPs, USP19, was previously shown to regulate the stability of the cell cycle regulator $p27^{Kip}$ and to rescue the substrates of endoplasmic reticulum-associated degradation (36, 37). In this study, we identify USP19 as a c-IAP1 and 2-interacting protein. USP19 prevents ubiquitination of c-IAP1 and c-IAP2 and stabilizes them. Our finding reveals a role for DUBs in controlling the stability of the c-IAP ubiquitin E3 ligases.

EXPERIMENTAL PROCEDURES

Reagents and Plasmids—The following reagents were obtained from the indicated sources: antibodies against USP19 (Novus Biologicals), c-IAP1 (Enzo Life Sciences), c-IAP2 (BD Biosciences), and HA (Santa Cruz Biotechnology); anti-FLAG polyclonal antibody and monoclonal antibody M2, calpain inhibitor I (*N*-acetyl-Leu-Leu-nor-Leu-al, ALLN), MG132, iodoacetate, 3x-FLAG peptide, cycloheximide, and anti-FLAG M2 and anti-HA beads (Sigma); TNFα (R&D Systems); Lipofectamine 2000 (Invitrogen); tetra-ubiquitin (Biomol); complete EDTA free protease inhibitors (Roche Applied Science); FITC-conjugated anti-rabbit and rhodamine-conjugated anti-mouse IgG antibodies and Vectashield containing DAPI (Vector). USP19 cDNA was amplified from the DNA clone KIAA0891 (kindly provided by the human unidentified gene-encoded (HUGE) consortium of Japan) and cloned into the EcoRI and XhoI sites of pRK5 with a C-terminal FLAG or HA tag. The active site Cys-506 to Ala mutation and deletion mutations were generated by PCR and confirmed by DNA sequencing. Plasmids expressing XIAP, c-IAP1, c-IAP2, and various mutants were previously described (9, 25, 26).

Affinity Purification—The FLAG-tagged c-IAP2 BIR2 + 3 (amino acids 101–346) was expressed in HEK293T cells through transient transfection and purified to apparent homogeneity via anti-FLAG mAb M2 conjugated to agarose beads. The immobilized FLAG-c-IAP2 BIR protein was then incubated with the S100 fraction of HeLa S3 cells as described (38, 39). As a control, the HeLa S100 fraction was also incubated with the anti-FLAG beads. After extensive washing, the bound proteins were eluted, and proteins that specifically associated with FLAG-c-IAP2 BIR2 + 3 were analyzed by mass spectrometry at the Proteomic Core Facility of the Abramson Cancer Center at the University of Pennsylvania.

Sequence Analysis and Northern Blot—In the USP19 plasmid KIAA0891, an in-frame stop codon before the first ATG is not found in the sequence of USP19 but exists in a human EST clone containing additional nucleotides at the 5′ end (No. CB044698). Thus, the sequence in KIAA0891 is likely to be the full-length USP19 sequence. The entire open reading frame was sequenced. The protein domains of USP19 were analyzed by using the SMART program (available on-line). For Northern analysis, human 12-well multiple tissue (Clontech, catalogue no. 636818) and cancer cell line (Clontech, catalogue no. 636804) blots were hybridized with a [^{32}P]dCTP-labeled cDNA probe spanning the C-terminal segment (nucleotides 3140–3960) of the human USP19 open reading frame according to the manufacturer's instruction.

RNA Interference—USP19 shRNAs and control shRNA were purchased from Open Biosystems. To generate lentiviruses expressing USP19 and control shRNAs, HEK293T cells grown on a 6-cm dish were transfected with 2 μg of PLKO.1 USP19 shRNAs or control vector, 2 μg of pREV, 2 μg of pGag/Pol/PRE, and 1 μg of pVSVG. 24 h after transfection, cells were cultured with DMEM medium containing 20% FBS for an additional 24 h. The culture medium containing lentivirus particles was centrifuged at 1000 $\times$ *g* for 5 min, and viruses in the supernatant were used for infection.

Immunoprecipitation and Western Blot—HEK293T cells were transfected with the indicated plasmids. 24 h after transfection, cells were harvested and lysed in the IP lysis buffer (50 mM Tris-HCl, pH 7.4, 150 mM NaCl, 1.5 mM $MgCl_2$, 20 μM MG132, 10% glycerol, 1% Triton X-100, and protease inhibitors). The soluble fractions were incubated with anti-FLAG M2 or anti-HA beads for 2 h at 4 °C. The immunoprecipitates were then washed five times and resolved by SDS-PAGE followed by Western blot analysis using rabbit anti-FLAG or anti-HA antibody. To detect the interaction of endogenous USP19 and c-IAP2, Jurkat cells were treated with MG132 for 4 h. Cell lysates were incubated overnight at 4 °C with anti-USP19 antibody or control rabbit IgG antibody bound to protein A-agarose beads. The immunoprecipitated proteins were analyzed by Western blot with anti-USP19 and anti-c-IAP2 antibodies.

Immunofluorescence—HeLa cells grown on glass coverslips were transfected with indicated plasmids. 24 h after transfection, cells were washed once with PBS, fixed with 4% paraformaldehyde, and permeabilized with 0.01% Triton X-100 (in PBS). After being blocked with 1% BSA (in PBS) for 1 h, cells

were incubated at room temperature with anti-FLAG or anti-HA antibody for 1 h and with rhodamine-conjugated anti-mouse or FITC-conjugated anti-rabbit IgG secondary antibodies for an additional 1 h. The cells were washed twice with PBS containing 0.1% Tween 20, dried in 100% EtOH, and mounted with Vectashield containing DAPI. The cells were visualized by fluorescence microscopy (Leica).

In Vivo and in Vitro Deubiquitination Assays—HEK293T cells expressing FLAG-c-IAP2, FLAG-c-IAP2 and HA-USP19, or FLAG-c-IAP2 and HA-USP19 CA were lysed in 1% SDS (in 50 mM Tris-HCl, pH 7.6, and 120 mM NaCl) and boiled for 5 min at 100 °C. The lysates were diluted 1:10 in IP-lysis buffer and immunoprecipitated by anti-FLAG M2 beads as described above. The immunoprecipitated proteins were analyzed by Western blot with polyclonal anti-FLAG antibody. For *in vitro* deubiquitination experiments, FLAG-USP19 and FLAG-USP19 CA were expressed in HEK293T cells and purified as described (38, 39). The purified proteins were eluted with 150 ng/ml 3×FLAG peptide. The proteins were then incubated with tetra-ubiquitin (0.75 μg) in deubiquitination buffer (50 mM Tris-HCl, pH 7.4, 1 mM $MgCl_2$, and 1 mM DTT) at 37 °C for the indicated time. USP19 was also incubated in the presence of 5 mM iodoacetate. The samples were resolved on a 4–20% gradient gel and analyzed by Coomassie Blue staining. For c-IAP2 deubiquitination, modified c-IAP2 was purified from HEK293T cells that had been transfected for 24 h and treated with 20 μM ALLN for 4 h. After being eluted from M2 beads, c-IAP2 was incubated with USP19 and USP19 CA.

Apoptosis Assay—MDA-MB 231 cells expressing control shRNA or USP19 specific shRNA were treated with or without TNFα (20 ng/ml) for 20 h. Cells were stained with Hoechst 33342, and apoptosis was determined by counting the apoptotic cells with the aberrant nuclei staining.

Reproducibility—All data, with the exception of the initial affinity purification of IAP2-interacting proteins and the Northern blot analysis, are representatives of two to three independent experiments.

RESULTS

USP19 Interacts with c-IAPs and XIAP—To better understand the regulation of c-IAP stability, we sought to identify c-IAP2-interacting proteins using an affinity purification approach (38, 39). Because the BIR region is the main protein-interaction domain of IAPs, we expressed a FLAG-tagged c-IAP2 protein containing the second and third BIR domains (FLAG-c-IAP2 BIR2 + 3) in HEK293T cells and purified it to apparent homogeneity using anti-FLAG antibody. The FLAG-c-IAP2 BIR2 + 3 protein immobilized on beads was then incubated with S100 extract of HeLa S3 cells. Proteins that specifically bound to the c-IAP2 BIR2 + 3 beads, but not the control beads, were analyzed by mass spectrometry. One protein was found to be USP19. Like the other UBPs, USP19 contains the USP enzymatic domain with a conserved catalytic cysteine-histidine dyad. In addition, USP19 contains a transmembrane domain at the C terminus (supplemental Fig. S1) (37, 40).

To examine the expression profile of USP19 mRNA, a human multiple tissue Northern blot was hybridized with a radioisotope-labeled USP19 cDNA probe. A single transcript ~5 kb in size was detected in virtually all tissues examined, with high expression found in the heart, skeletal muscle, brain, kidney, and placenta; medium expression in the spleen, liver, small intestine, thymus, and leukocytes; and low expression in the colon and lung (supplemental Fig. S2). In addition, the USP19 transcript was detected in various human tumor cell lines with comparable levels of expression, except in lung carcinoma A539 and promyelocytic leukemia HL60 cells where less expression was observed (supplemental Fig. S2).

To confirm the interaction of c-IAP2 with USP19, FLAG-tagged c-IAP2 was expressed together with HA-tagged USP19 in HEK293T cells. A co-immunoprecipitation assay using anti-HA antibody showed a specific interaction between these two proteins (Fig. 1*A* and supplemental Fig. S3*A*). The interaction was verified in a reciprocal co-immunoprecipitation experiment using anti-FLAG antibody (Fig. 1*B*). We next examined the interaction between endogenous c-IAP2 and USP19. When lysates from Jurkat cells were incubated separately with anti-USP19 antibody and a control antibody, c-IAP2 was detected in the anti-USP19, but not the control, immunoprecipitates (Fig. 1*C*). The specificity of the anti-c-IAP2 antibody was underscored by the observation that, when cells were treated with the Smac mimetics BV6, the detected c-IAP2 signal rapidly disappeared as expected (20) (supplemental Fig. S3*B*). Taken together, these results indicate that c-IAP2 interacts with USP19. Given the structural similarity between c-IAP2 and c-IAP1, we tested whether c-IAP1 binds to USP19. As shown in Fig. 1*A*, c-IAP1 also interacted with USP19, but not as strongly as c-IAP2 (Fig. 1*A*). In addition, XIAP associated with USP19 (Fig. 1*B*).

We next examined whether USP19 co-localizes with c-IAP2. When expressed individually, c-IAP2 mainly localized in the nucleus, whereas USP19 was exclusively associated with cytoplasmic structures resembling endoplasmic reticulum membrane, consistent with previously reports (37, 41). In the presence of USP19, c-IAP2 was re-localized to the cytoplasm, exhibiting a localization pattern similar to USP19 (Fig. 1*D*). This result indicates the interaction of USP19 and c-IAP2 in cells.

Structural Determinants of the c-IAP2-USP19 Interaction—To delineate the structural determinants of the c-IAP2-USP19 interaction, we used a panel of c-IAP2 and USP19 mutants (Fig. 2*A*). The c-IAP2 N-terminal region containing all three BIR domains (*N*) showed a strong interaction with USP19, whereas the C-terminal region containing the CARD and RING domains (*C*) showed no interaction (Fig. 2*B*). Furthermore, deletion of either the BIR1 (ΔN100 and BIR2 + 3) or the BIR3 (BIR1 + 2) domain didn't affect the c-IAP2-USP19 interaction (Fig. 2*C*). Therefore, the c-IAP2 BIR2 domain likely mediates the interaction of c-IAP2 with USP19.

USP19 contains a ubiquitin-specific protease domain in its C terminus that includes a catalytic Cys residue at amino acid 506 (Fig. 2*A*). Mutation of this Cys to Ala (CA) did not impair the interaction of USP19 with c-IAP2 N (Figs. 1*B* and 2*D*). Furthermore, both the region N-terminal to the USP domain (*N*) and the region containing the USP and the transmembrane domain (*C*) were able to associate with c-IAP2 N (Fig. 2*D*). For these

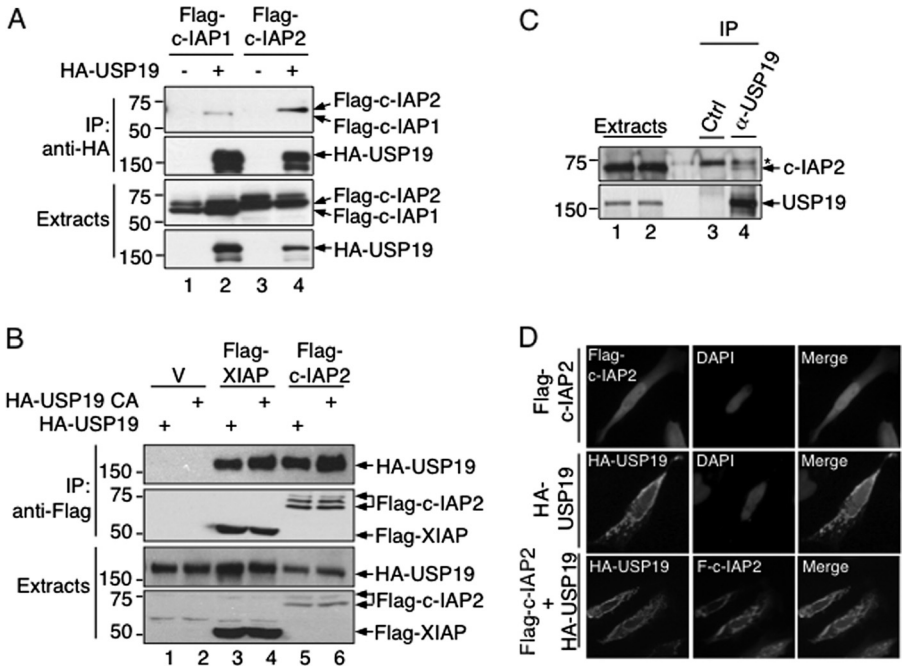

FIGURE 1. **USP19 interacts with c-IAP1, c-IAP2, and XIAP.** *A*, interaction of USP19 with c-IAPs. FLAG-tagged c-IAP1 or c-IAP2 was transfected into HEK293T cells either alone or together with HA-USP19. Cell lysates were immunoprecipitated with anti-HA beads. The immunoprecipitates and input extracts were analyzed by Western blot. *B*, interaction of USP19 with c-IAP2 and XIAP. HA-USP19 or HA-USP19 CA was transfected into HEK293T cells together with vector control (*V*), FLAG-XIAP, or FLAG-c-IAP2. Cell lysates were subjected to immunoprecipitation with anti-FLAG M2 beads followed by Western blot analysis. *C*, interaction of endogenous USP19 and c-IAP2. Jurkat cell lysates were subjected to immunoprecipitation with anti-USP19 antibody. Immunoprecipitates were analyzed by Western blot using anti-c-IAP2 antibody. *, a nonspecific band. *D*, co-localization of exogenous USP19 and c-IAP2. HeLa cells expressing FLAG-c-IAP2 and HA-USP19 individually or in combination were immunostained with anti-FLAG and/or anti-HA antibody followed by Rhodamine-conjugated anti-mouse and/or FITC-conjugated anti-rabbit IgG.

experiments, c-IAP2 N was used due to a more stable expression level compared with full-length c-IAP2. These data suggest that both N- and C-terminal regions of USP19 interact with c-IAP2.

USP19 Deubiquitinates c-IAP2 in Vitro and Prevents c-IAP2 Ubiquitination in Vivo through Both DUB-dependent and -independent Mechanisms—To confirm the deubiquitinase activity of USP19, we purified FLAG-USP19 to apparent homogeneity and incubated it with a tetra-ubiquitin chain. As shown in Fig. 3*A*, USP19, but not USP19 CA, cleaved the tetra-ubiquitin chain to mono-ubiquitin. The activity of USP19 was blocked by iodoacetate, a cysteine-specific alkylating agent that inhibits deubiquitinating enzymes.

To determine whether USP19 can remove ubiquitin from conjugated c-IAP2, poly-ubiquitinated c-IAP2 was generated by transiently overexpressing FLAG-c-IAP2 in HEK293T cells in the presence of the proteasome inhibitor ALLN and subsequently affinity-purified. The purified c-IAP2 protein was almost completely deubiquitinated by the purified USP19 protein (Fig. 3*B*). Again, this activity of USP19 was abolished by iodoacetate, and USP19 CA showed no DUB activity on ubiquitinated c-IAP2.

We next investigated the effect of USP19 on c-IAP2 ubiquitination *in vivo*. c-IAP2 was strongly self-ubiquitinated upon overexpression in HEK293T cells. However, when co-expressed with USP19, c-IAP2 ubiquitination was virtually abolished (Fig. 3*C*). Interestingly, USP19 CA also inhibited c-IAP2 ubiquitination, although to a lesser extent compared with USP19. Because USP19 CA lacked any detectable deubiquitinating enzyme activity (Fig. 3, *A* and *B*), it likely reduces c-IAP2 ubiquitination through a DUB-independent mechanism.

USP19 Stabilizes c-IAP1 and c-IAP2—To examine the effect of USP19 on the expression of endogenous c-IAP1 and c-IAP2, we knocked down USP19 in HeLa and MDA-MB231 cells using small hairpin (sh) RNA. This led to a significant decrease in the levels of endogenous c-IAP2 and, to a lesser extent, the level of endogenous c-IAP1 (Fig. 4*A*). Knockdown of USP19 also reduced endogenous c-IAP2 levels in Jurkat cells (supplemental Fig. S3*C*). Next we increased the amount of USP19 through transient transfection. Upon overexpression, USP19 markedly increased the levels of c-IAP2 (Fig. 4*B*). Notably, the DUB-deficient USP19 CA similarly increased c-IAP2 levels. To determine whether USP19 prolonged the half-life of c-IAP proteins, FLAG-c-IAP1 and FLAG-c-IAP2 were expressed alone and together with HA-USP19 or HA-USP19 CA, and cells were treated with the protein synthesis inhibitor cycloheximide for variable lengths of time. c-IAP1 and c-IAP2 were strongly stabilized by both USP19 and USP19 CA (Fig. 4*C*). In contrast, USP19 and USP19 CA did not influence the stability of the tumor suppressor p53 (Fig. 4*C*), which is a labile protein, underscoring the specific effect of USP19 and USP19 CA on c-IAPs. Conversely, knockdown of USP19 by shRNA noticeably shortened the half-life of both endogenous c-IAP1 and c-IAP2 (Fig. 4*D*). Taken together, these results show that USP19 controls the stability of c-IAP1 and c-IAP2. Moreover, the effect of USP19 overexpression on c-IAP stability is largely independent of its DUB activity.

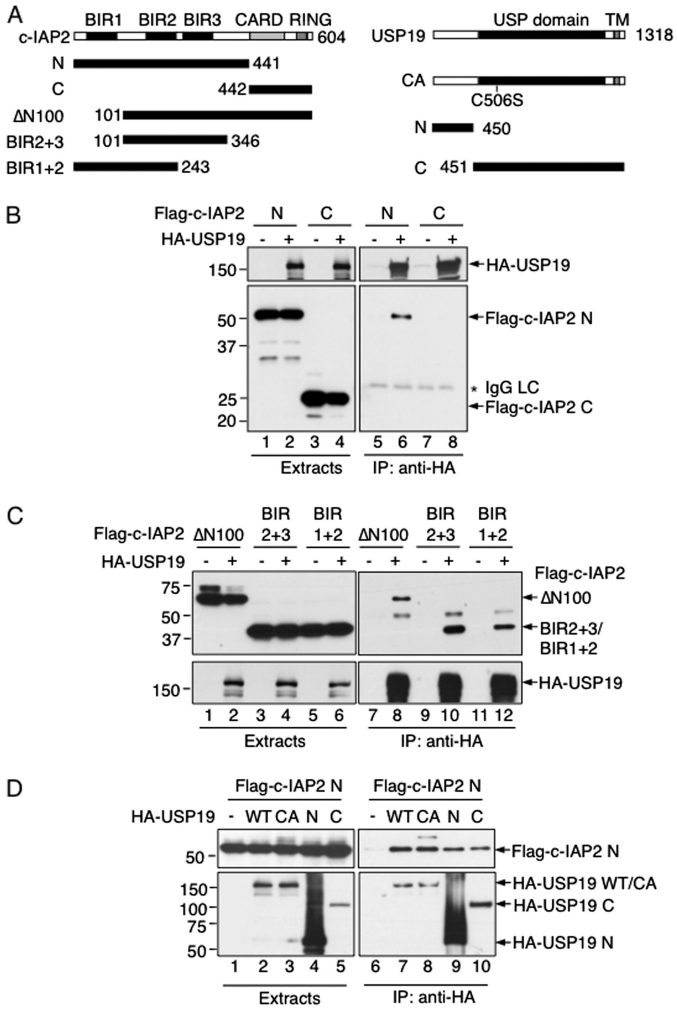

FIGURE 2. **Structural determinants of the USP19-c-IAP2 interaction.** *A*, schematic representation of c-IAP2 (*left*), USP19 (*right*), and their mutants used in this work. *B* and *C*, each of the indicated c-IAP2 mutants was expressed in HEK293T cells alone or together with HA-USP19. Cell lysates were immunoprecipitated with anti-HA beads. The immunoprecipitates and extracts were analyzed by Western blot. *D*, FLAG-c-IAP2 N was expressed in HEK293T cells alone or together with the indicated HA-USP19 proteins. Cell lysates were analyzed as in *B* and *C*.

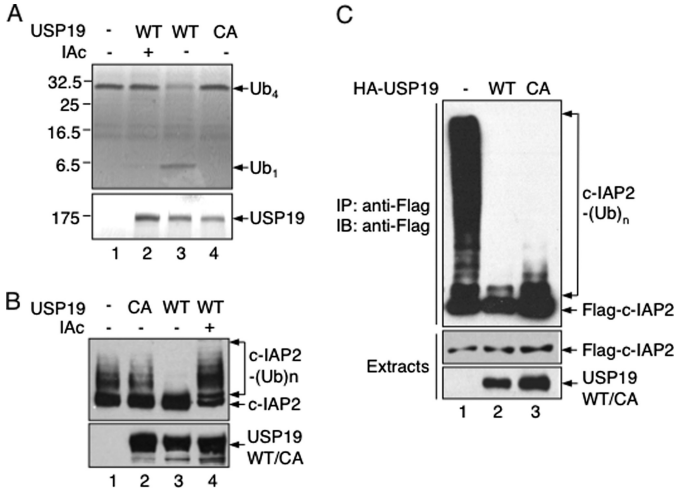

FIGURE 3. **Deubiquitination of c-IAP2 by USP19.** *A*, *in vitro* deubiquitination assay. Tetra-Ub peptide was treated with recombinant USP19 or USP19 CA in the presence or absence of iodoacetate (*IAc*). Samples were analyzed by SDS-PAGE and Coomassie Blue staining. *B*, ubiquitinated FLAG-c-IAP2 protein was treated with USP19 WT and USP19 CA in the presence (+) or absence (−) of iodoacetate (*IAc*). Reaction mixes were analyzed by Western blot. *C*, FLAG-c-IAP2 was co-expressed with vector control (−), HA-USP19, or HA-USP19 CA in HEK293T cells. c-IAP2 was immunoprecipitated with anti-FLAG M2 beads and detected by a polyclonal anti-FLAG antibody. Lysates were blotted for c-IAP2 with M2 and for USP19 with anti-HA antibody.

USP19 Associates with Itself and Is Stabilized by Its Own Deubiquitinase Activity—Given that USP19 does not seem to rely on its DUB activity to stabilize c-IAPs (Fig. 4, *B* and *C*), we asked whether the DUB activity of USP19 plays a role in regulating its own ubiquitination. When expressed together with HA-ubiquitin in HEK293T cells, USP19 CA was readily ubiquitinated (Fig. 5*A*). This ubiquitination was further enhanced upon treatment with the proteasome inhibitor ALLN. In contrast, no ubiquitination was detected on USP19 even in the presence of ALLN. Therefore, USP19 likely removes associated ubiquitin moieties via self-deubiquitination. Correlating with their ubiquitination status, USP19 was noticeably more stable than USP19 CA (Fig. 5*B*). To investigate how USP19 might be stabilized by its de-ubiquitinase activity, we tested whether USP19 can self-interact. FLAG-USP19 was expressed with HA-USP19 or HA-USP19 CA in HEK293T cells. An immunoprecipitation assay showed that FLAG-USP19 could associate with both HA-USP19 and HA-USP19 CA (Fig. 5*C*). In contrast, USP19 did not interact with another DUB, USP7/HAUSP (supplemental Fig. S3*D*). As expected from the ability of USP19 to self-interact, USP19 increased the levels of USP19 CA in a dose-dependent manner when they were co-expressed in cells (Fig. 5*D*). Collectively, these results suggested that USP19 stabilizes itself through self-association and intermolecular deubiquitination.

USP19 Inhibits TNFα-induced Apoptosis via the Stabilization of c-IAPs—c-IAPs inhibit TNFα-mediated apoptosis, a property underlying the cytotoxic effect of Smac mimetics in cancer cells (20, 21, 31, 32). To examine the physiological significance of USP19-mediated stabilization of c-IAPs, USP19 was knocked down in MDA-MB231 breast cancer cells. Compared with control cells, USP19 knockdown cells showed elevated levels of apoptosis (from 10% to 21%) in response to treatment with TNFα (Fig. 6*A*, *lane 4 versus 2*). Accordingly, USP19 knockdown cells also exhibited higher levels of caspase-8 activation and poly(ADP-ribose) polymerase cleavage compared with control cells. TNFα treatment effectively increased the levels of c-IAPs, particularly c-IAP2. This increase was likely due to TNFα-mediated activation of NF-κB, which controls the expression of c-IAPs (42). Nevertheless, the increase in IAP expression was less in USP19 knockdown cells compared with control cells (Fig. 6*A*). To further test whether USP19 may have an anti-apoptotic function through stabilizing c-IAP1 and c-IAP2, FLAG-c-IAP1 and FLAG-c-IAP2 were individually transfected into the USP19 knockdown and control cells. Both c-IAP1 and c-IAP2 prevented the increase in TNFα-induced apoptosis caused by USP19 knockdown (Fig. 6*B*, *lanes 12* and *10 versus 8*). c-IAP1 and c-IAP2 also decreased TNFα-induced poly(ADP-ribose) polymerase cleavage and caspase-8 activation in USP19 knockdown cells. Compared with

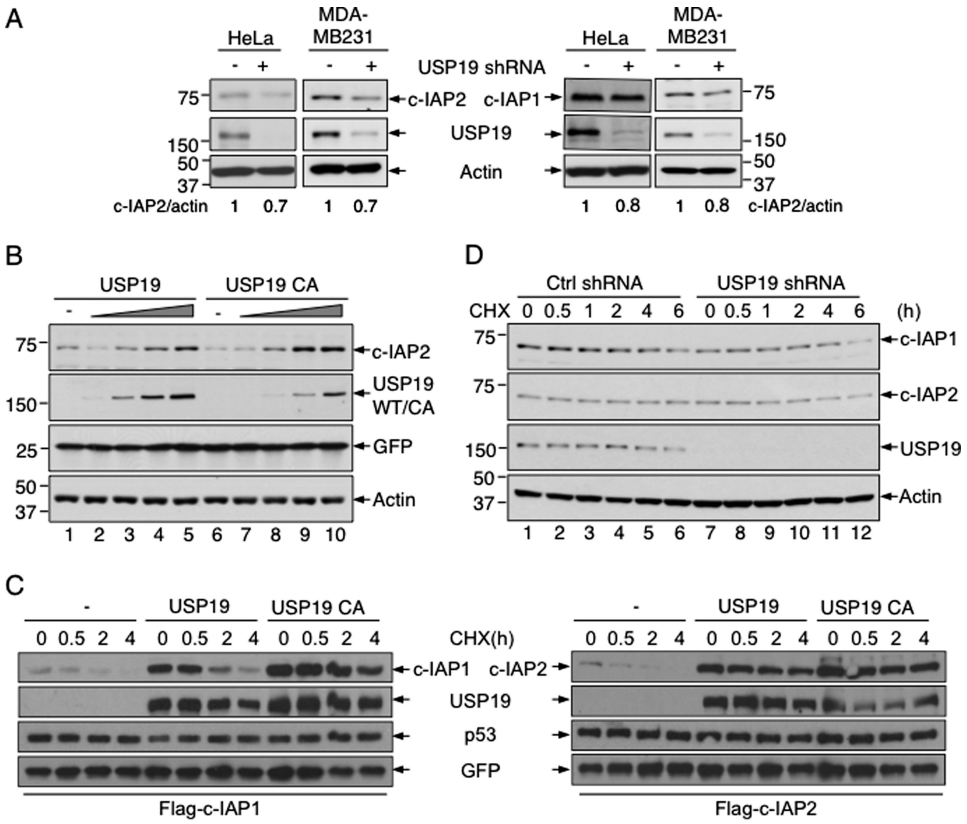

FIGURE 4. **USP19 stabilizes c-IAPs.** *A*, HeLa and MDA-MB231 cells were infected with lentiviruses expressing a control shRNA (−) or USP19 shRNA. Protein expression was analyzed by Western blot. Protein bands were quantified by NIH image software, and relative ratios of c-IAP1 or c-IAP2 *versus* actin are indicated. *B*, Western blot analysis of HeLa cells transfected with FLAG-c-IAP2 and increasing amounts of HA-USP19 or HA-USP19 CA. GFP was included as a control for transfection efficiency. *C*, HEK293T cells were transfected with FLAG-c-IAP1 (*left*) or FLAG-c-IAP2 (*right*), and vector (−), HA-USP19, or HA-USP19 CA. p53 and GFP were included as controls. Cells were treated with cycloheximide for the indicated periods of time and analyzed by Western blot. *D*, MDA-MB231 cells infected with the lentivirus expressing control shRNA (−) or USP19 shRNA were treated with cycloheximide (*CHX*) for the indicated periods of time and analyzed by Western blot.

c-IAP2, c-IAP1 was less potent in reversing apoptosis that was caused by USP19 knockdown, consistent with their relative binding strengths to USP19 (Fig. 1*A*). Taken together, these data suggest that USP19-mediated stabilization of c-IAPs inhibits TNFα-induced apoptosis.

DISCUSSION

c-IAP1 and 2 are ubiquitin ligases that regulate the stability of a variety of apoptotic and non-apoptotic proteins. An intriguing issue remains on how ubiquitination and proteasomal degradation of c-IAPs are normally prevented. The current study identifies USP19 as a stabilizer for c-IAPs with the consequential inhibition of apoptosis, revealing a role for a deubiquitinating enzyme in the regulation of IAP stability. Stabilization of ubiquitin E3 ligases by deubiquitinating enzymes has been suggested by previous studies. For example, the stability of Mdm2, an oncogenic E3 ligase and the major antagonist of the tumor suppressor p53, is controlled by the deubiquitinating enzyme HAUSP via the adaptor protein Daxx (39). USP19-mediated stabilization of c-IAPs further underscores the dynamic interplay between ubiquitin ligases and deubiquitinating enzymes.

Notably, USP19 appears to stabilize c-IAPs through a protease-independent mechanism, at least upon overexpression (Figs. 3 and 4). The precise nature remains to be determined, but conceivably, USP19 might mask Lys residues on c-IAPs that are critical for ubiquitination or prevent the binding of a ubiquitin conjugating enzyme (E2) to c-IAPs. Regardless, this deubiquitinase-independent mechanism may be important considering that c-IAPs, like other E3 ligases, could in theory constantly self-ubiquitinate. By blocking the self-addition of ubiquitin, USP19 would effectively prevent a futile cycle of ubiquitination and deubiquitination. The deubiquitinating activity might then reverse any small amount of ubiquitination, functioning as a fail-safe mechanism to prevent aberrant activation of apoptosis. It will be interesting to determine whether other deubiquitinating enzymes also function in a similar manner to prevent the self-ubiquitination of E3 ligases. The deubiquitinase activity of USP19 does appear to control its own stability, which is facilitated by dimerization or oligomerization (Fig. 5), and thus may indirectly affect c-IAP levels.

Among the c-IAPs, c-IAP2 appears to be a major target of USP19. Despite their high structural homology, c-IAP1 and c-IAP2 have overlapping and distinct targets and functions. For example, c-IAP1, but not c-IAP2, mediates the ubiquitination of TRAF2 and Mad1 (8, 27), whereas only c-IAP2 is involved in MALT lymphomas (25, 26). The preferential binding of USP19 to c-IAP2 suggests that the stability of c-IAPs may be differen-

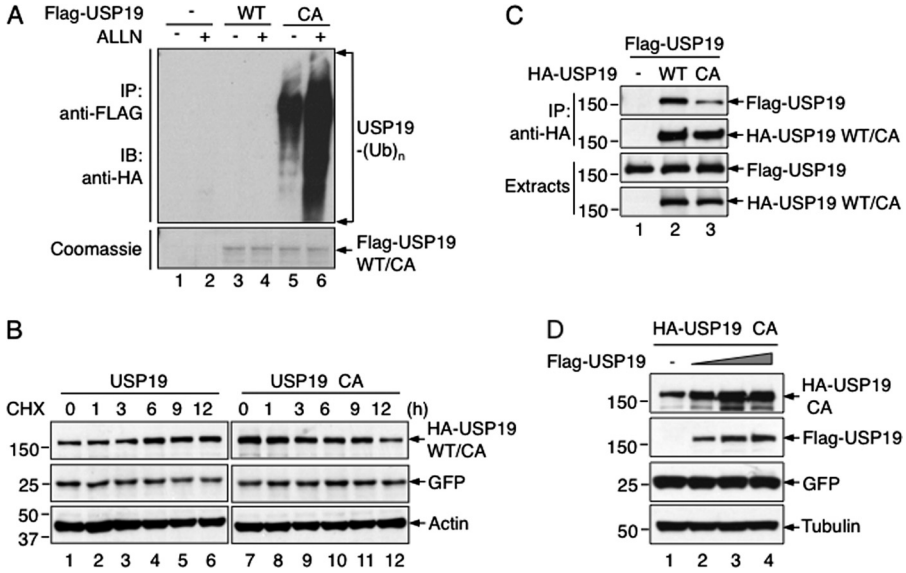

FIGURE 5. **Auto-deubiquitination and self-interaction of USP19.** *A*, HEK293 cells were transfected with HA-Ub plus vector control, FLAG-USP19, or FLAG-USP19 CA. Cells were treated with or without 20 μM ALLN. FLAG-tagged proteins were immunoprecipitated and analyzed by Western blotting with anti-HA antibody (*top*) and Coomassie Blue staining (*bottom*). *B*, Western blot analysis of HeLa cells transfected with HA-USP19 or HA-USP19 CA and treated with cycloheximide (*CHX*) for the indicated periods of time. *C*, FLAG-USP19 was expressed in HEK293T cells alone or together with HA-USP19 or HA-USP19 CA. Cell extracts were immunoprecipitated with anti-HA antibody. Extracts and immunoprecipitates were analyzed by Western blot. Actin and GFP levels are shown as sample loading and transfection efficiency controls, respectively. *D*, HEK293T cells were transfected with HA-USP19 CA plus increasing amounts of FLAG-USP19 (0, 0.25, 0.5, and 1 μg). Cell extracts were analyzed by Western blot.

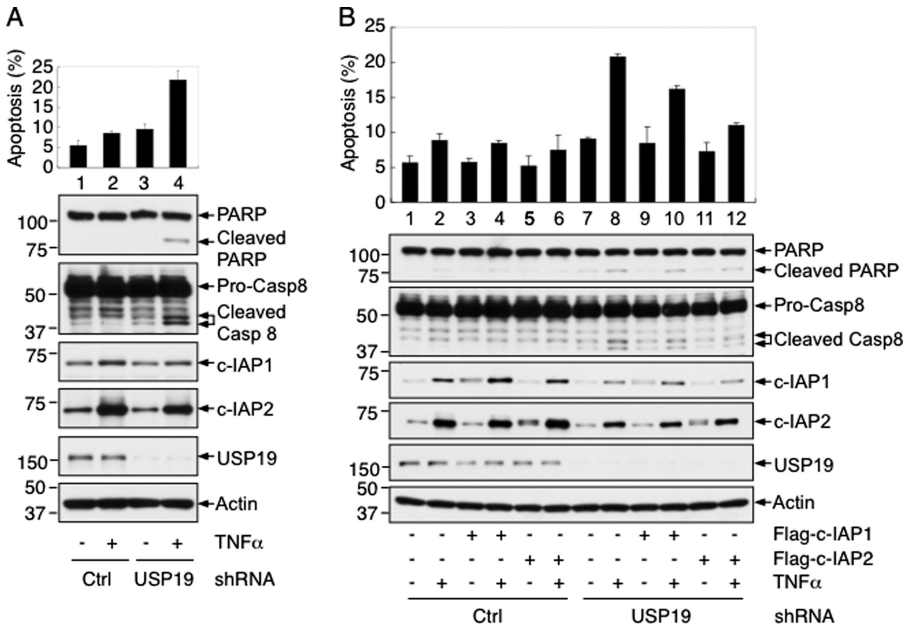

FIGURE 6. **Down-regulation of USP19 enhances TNFα-induced apoptosis.** *A* and *B*, MDA-MB231 cells expressing control shRNA or USP19 shRNA were treated with TNFα (20 ng/ml) for 20 h (*A*) or transfected with control vector (−), FLAG-c-IAP1, and FLAG-c-IAP2, and then treated with TNFα (*B*). *Top panel*: Percentages of apoptotic cells shown as the mean ± S.D. of three independent experiments. *Bottom panels*: expression of proteins, activation of caspase-8, and cleavage of poly(ADP-ribose) polymerase in cell extracts analyzed by Western blot.

tially regulated. Although XIAP can also interact with USP19, the consequence of this interaction is currently unclear because XIAP is a much weaker E3 ligase compared with c-IAP1 and c-IAP2 (9) and may rely less on a deubiquitinating enzyme for stabilization. However, it remains possible that, by binding to XIAP (and c-IAPs), USP19 might influence the ubiquitination status of the IAP targets.

Currently, IAP antagonists, such as compounds mimicking the IAP antagonist Smac/DIABLO, are being extensively investigated as a treatment for cancer. Although Smac was thought to mainly inhibit XIAP, Smac mimetics induce c-IAP degradation and generate autocrine TNFα apoptotic signaling (20, 21, 31, 32). However, the efficacy of these mimetics varies among different tumors (31), and the cause of this variation is a highly important, yet poorly understood, issue. It will be interesting to determine whether USP19 influences the effectiveness of Smac mimetics in cancer therapy.

Acknowledgments—We thank the human unidentified gene-encoded (HUGE) consortium of Japan for providing the USP19 cDNA (clone KIAA0891), Genentech Inc. and Dr. X. Wang for Smac mimetics, Dr. A. Minn for MDA-MB231 cells, the National Cell Culture Center for HeLa S3 cells, and UPenn Abramson Cancer Center Proteomic Core for mass spectrometry analysis.

REFERENCES

1. Crook, N. E., Clem, R. J., and Miller, L. K. (1993) *J. Virol.* **67,** 2168–2174
2. Birnbaum, M. J., Clem, R. J., and Miller, L. K. (1994) *J. Virol.* **68,** 2521–2528
3. Salvesen, G. S., and Duckett, C. S. (2002) *Nat. Rev. Mol. Cell Biol.* **3,** 401–410
4. Vaux, D. L., and Silke, J. (2005) *Nat. Rev. Mol. Cell Biol.* **6,** 287–297
5. Srinivasula, S. M., and Ashwell, J. D. (2008) *Mol. Cell* **30,** 123–135
6. Gyrd-Hansen, M., and Meier, P. (2010) *Nat. Rev. Cancer* **10,** 561–574
7. Yang, Y., Fang, S., Jensen, J. P., Weissman, A. M., and Ashwell, J. D. (2000) *Science* **288,** 874–877
8. Li, X., Yang, Y., and Ashwell, J. D. (2002) *Nature* **416,** 345–347
9. Hu, S., and Yang, X. (2003) *J. Biol. Chem.* **278,** 10055–10060
10. Deveraux, Q. L., Takahashi, R., Salvesen, G. S., and Reed, J. C. (1997) *Nature* **388,** 300–304
11. Chang, H. Y., and Yang, X. (2000) *Microbiol. Mol. Biol. Rev.* **64,** 821–846
12. Li, J., and Yuan, J. (2008) *Oncogene* **27,** 6194–6206
13. Ryoo, H. D., Bergmann, A., Gonen, H., Ciechanover, A., and Steller, H. (2002) *Nat. Cell Biol.* **4,** 432–438
14. Schile, A. J., García-Fernández, M., and Steller, H. (2008) *Genes Dev.* **22,** 2256–2266
15. Rothe, M., Pan, M. G., Henzel, W. J., Ayres, T. M., and Goeddel, D. V. (1995) *Cell* **83,** 1243–1252
16. Du, C., Fang, M., Li, Y., Li, L., and Wang, X. (2000) *Cell* **102,** 33–42
17. Verhagen, A. M., Ekert, P. G., Pakusch, M., Silke, J., Connolly, L. M., Reid, G. E., Moritz, R. L., Simpson, R. J., and Vaux, D. L. (2000) *Cell* **102,** 43–53
18. Bertrand, M. J., Milutinovic, S., Dickson, K. M., Ho, W. C., Boudreault, A., Durkin, J., Gillard, J. W., Jaquith, J. B., Morris, S. J., and Barker, P. A. (2008) *Mol. Cell* **30,** 689–700
19. Mahoney, D. J., Cheung, H. H., Mrad, R. L., Plenchette, S., Simard, C., Enwere, E., Arora, V., Mak, T. W., Lacasse, E. C., Waring, J., and Korneluk, R. G. (2008) *Proc. Natl. Acad. Sci. U.S.A.* **105,** 11778–11783
20. Varfolomeev, E., Blankenship, J. W., Wayson, S. M., Fedorova, A. V., Kayagaki, N., Garg, P., Zobel, K., Dynek, J. N., Elliott, L. O., Wallweber, H. J., Flygare, J. A., Fairbrother, W. J., Deshayes, K., Dixit, V. M., and Vucic, D. (2007) *Cell* **131,** 669–681
21. Vince, J. E., Wong, W. W., Khan, N., Feltham, R., Chau, D., Ahmed, A. U., Benetatos, C. A., Chunduru, S. K., Condon, S. M., McKinlay, M., Brink, R., Leverkus, M., Tergaonkar, V., Schneider, P., Callus, B. A., Koentgen, F., Vaux, D. L., and Silke, J. (2007) *Cell* **131,** 682–693
22. Zarnegar, B. J., Wang, Y., Mahoney, D. J., Dempsey, P. W., Cheung, H. H., He, J., Shiba, T., Yang, X., Yeh, W. C., Mak, T. W., Korneluk, R. G., and Cheng, G. (2008) *Nat. Immunol.* **9,** 1371–1378
23. Vallabhapurapu, S., Matsuzawa, A., Zhang, W., Tseng, P. H., Keats, J. J., Wang, H., Vignali, D. A., Bergsagel, P. L., and Karin, M. (2008) *Nat. Immunol.* **9,** 1364–1370
24. Isaacson, P. G., and Du, M. Q. (2004) *Nat. Rev. Cancer* **4,** 644–653
25. Hu, S., Du, M. Q., Park, S. M., Alcivar, A., Qu, L., Gupta, S., Tang, J., Baens, M., Ye, H., Lee, T. H., Marynen, P., Riley, J. L., and Yang, X. (2006) *J. Clin. Invest.* **116,** 174–181
26. Hu, S., Alcivar, A., Qu, L., Tang, J., and Yang, X. (2006) *Cell Cycle* **5,** 1438–1442
27. Xu, L., Zhu, J., Hu, X., Zhu, H., Kim, H. T., LaBaer, J., Goldberg, A., and Yuan, J. (2007) *Mol. Cell* **28,** 914–922
28. Yang, Q. H., and Du, C. (2004) *J. Biol. Chem.* **279,** 16963–16970
29. Cheung, H. H., Plenchette, S., Kern, C. J., Mahoney, D. J., and Korneluk, R. G. (2008) *Mol. Biol. Cell* **19,** 2729–2740
30. Conze, D. B., Albert, L., Ferrick, D. A., Goeddel, D. V., Yeh, W. C., Mak, T., and Ashwell, J. D. (2005) *Mol. Cell. Biol.* **25,** 3348–3356
31. Petersen, S. L., Wang, L., Yalcin-Chin, A., Li, L., Peyton, M., Minna, J., Harran, P., and Wang, X. (2007) *Cancer Cell* **12,** 445–456
32. Wang, L., Du, F., and Wang, X. (2008) *Cell* **133,** 693–703
33. Fesik, S. W. (2005) *Nat. Rev. Cancer* **5,** 876–885
34. Nijman, S. M., Luna-Vargas, M. P., Velds, A., Brummelkamp, T. R., Dirac, A. M., Sixma, T. K., and Bernards, R. (2005) *Cell* **123,** 773–786
35. Komander, D., Clague, M. J., and Urbé, S. (2009) *Nat. Rev. Mol. Cell Biol.* **10,** 550–563
36. Lu, Y., Adegoke, O. A., Nepveu, A., Nakayama, K. I., Bedard, N., Cheng, D., Peng, J., and Wing, S. S. (2009) *Mol. Cell. Biol.* **29,** 547–558
37. Hassink, G. C., Zhao, B., Sompallae, R., Altun, M., Gastaldello, S., Zinin, N. V., Masucci, M. G., and Lindsten, K. (2009) *EMBO Rep.* **10,** 755–761
38. Tang, J., Wu, S., Liu, H., Stratt, R., Barak, O. G., Shiekhattar, R., Picketts, D. J., and Yang, X. (2004) *J. Biol. Chem.* **279,** 20369–20377
39. Tang, J., Qu, L. K., Zhang, J., Wang, W., Michaelson, J. S., Degenhardt, Y. Y., El-Deiry, W. S., and Yang, X. (2006) *Nat. Cell Biol.* **8,** 855–862
40. Combaret, L., Adegoke, O. A., Bedard, N., Baracos, V., Attaix, D., and Wing, S. S. (2005) *Am. J. Physiol. Endocrinol. Metab.* **288,** E693-E700
41. Samuel, T., Okada, K., Hyer, M., Welsh, K., Zapata, J. M., and Reed, J. C. (2005) *Cancer Res.* **65,** 210–218
42. Wang, C. Y., Mayo, M. W., Korneluk, R. G., Goeddel, D. V., and Baldwin, A. S., Jr. (1998) *Science* **281,** 1680–1683